ACS OMEGA

Article

Cite This: ACS Omega XXXX, XXX, XXX−XXX

http://pubs.acs.org/journal/acsodf

Design of a Helical-Stabilized, Cyclic, and Nontoxic Analogue of the Peptide Cm-p5 with Improved Antifungal Activity

Fidel E. Morales Vicente,[†,∥,▽] Melaine González-Garcia,[§] Erbio Diaz Pico,[∥] Elena Moreno-Castillo,[‡] Hilda E. Garay,[∥] Pablo E. Rosi,[#] Asiel Mena Jimenez,[‡] Jose A. Campos-Delgado,[▽] Daniel G. Rivera,[‡] Glay Chinea,[∥] Rosemeire C. L. R. Pietro,[○] Steffen Stenger,[⊥] Barbara Spellerberg,[⊥] Dennis Kubiczek,[¶] Nicholas Bodenberger,[¶] Steffen Dietz,[¶] Frank Rosenau,[¶] Márcio Weber Paixão,[*,▽] Ludger Ständker,[*,◆] and Anselmo J. Otero-González[*,§]

[†]General Chemistry Department, Faculty of Chemistry and [‡]Center for Natural Products Research, Faculty of Chemistry, University of Havana, Zapata y G, 10400 La Habana, Cuba

[§]Center for Protein Studies, Faculty of Biology, University of Havana, 25 and I, 10400 La Habana, Cuba

[∥]Synthetic Peptides Group, Center for Genetic Engineering and Biotechnology, P.O. Box 6162, 10600 La Habana, Cuba

[⊥]Institute of Medical Microbiology and Hygiene, University Clinic of Ulm, Robert Koch Str. 8, Ulm D-89081, Germany

[#]Department of Inorganic Chemistry, Analytical and Physical Chemistry, Facultad de Ciencias Exactas y Naturales, Universidad de Buenos Aires, Buenos Aires C1428EGA, Argentina

[▽]Center of Excellence for Research in Sustainable Chemistry (CERSusChem), Department of Chemistry, Federal University of São Carlos-UFSCar, São Paulo 13565-905, Brazil

[○]Laboratory of Pharmaceutical Biotechnology, Department of Drugs and Medicines, School of Pharmaceutical Sciences, UNESP, Araraquara 14800-900, Brazil

[◆]Core Facility for Functional Peptidomics, Ulm Peptide Pharmaceuticals (U-PEP), University Ulm, Faculty of Medicine, Ulm University, 89081 Ulm, Germany

[¶]Institute of Pharmaceutical Biotechnology, Ulm University, James-Frank-Ring N27, 89081 Ulm, Germany

Supporting Information

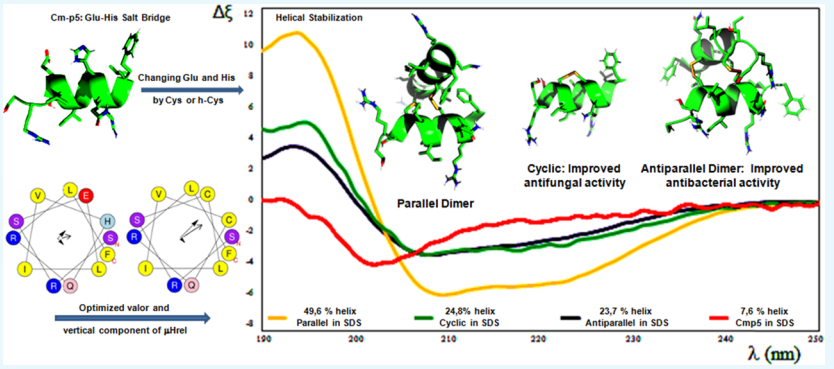

ABSTRACT: Following the information obtained by a rational design study, a cyclic and helical-stabilized analogue of the peptide Cm-p5 was synthetized. The cyclic monomer showed an increased activity in vitro against *Candida albicans* and *Candida parapsilosis*, compared to Cm-p5. Initially, 14 mutants of Cm-p5 were synthesized following a rational design to improve the antifungal activity and pharmacological properties. Antimicrobial testing showed that the activity was lost in each of these 14 analogues, suggesting, as a main conclusion, that a Glu−His salt bridge could stabilize Cm-p5 helical conformation during the interaction with the plasma membrane. A derivative, obtained by substitution of Glu and His for Cys, was synthesized and oxidized with the generation of a cyclic monomer with improved antifungal activity. In addition, two dimers were generated during the oxidation procedure, a parallel and antiparallel one. The dimers showed a helical secondary structure in water, whereas the cyclic monomer only showed this conformation in SDS. Molecular dynamic simulations confirmed the

continued...

Received: July 24, 2019
Accepted: October 4, 2019

DOI: 10.1021/acsomega.9b02201
ACS Omega XXXX, XXX, XXX−XXX

helical stabilizations for all of them, therefore indicating the possible essential role of the Glu−His salt bridge. In addition, the antiparallel dimer showed a moderate activity against *Pseudomonas aeruginosa* and a significant activity against *Listeria monocytogenes*. Neither the cyclic monomer nor the dimers were toxic against macrophages or THP-1 human cells. Due to its increased capacity for fungal control compared to fluconazole, its low cytotoxicity, together with a stabilized α-helix and disulfide bridges, that may advance its metabolic stability, and in vivo activity, the new cyclic Cm-p5 monomer represents a potential systemic antifungal therapeutic candidate.

INTRODUCTION

It has become apparent that an urgent need for developing new therapeutic principles and/or cures for infectious diseases exist, seeing the lack of new class of conventional antibiotics.[1] Bacterial and fungal resistance to antibiotic is a great issue for medicine nowadays, and the expected consequences of microbial resistant strains[2] may include detrimental effects in the brain, neurons (Alzheimer's disease and multiple sclerosis),[3] and biofilm formation in ear canal and teeth.[4]

In addition, abuse in the usage of antibiotics has been proposed as a drawback for natural microbiote, causing many and unexpected immunological, gastric, neurological, and opportunist microorganism disorders. In the same sense, antifungal or antibacterial drugs for systemic treatment are always accompanied by many side effects, making medical follow-ups of each case necessary.[5]

Antimicrobial peptides (AMPs) have been found in a wide range of organisms. They can act as part of the innate defense system of plants, vertebrates, and invertebrates against infections.[6] In general, they have the ability to directly kill microbes. However, in recent years, the concept for this heterogeneous group has been extended to host defense peptides. This is due to their abilities to disturb growth and also to modulate the immune system.[7] Immunomodulation and, in some cases, "beneficial immunogenicity" are extraordinary features that are not reachable by traditional antibiotics because their chemical nature is functionally incompatible with the immune system.

Notably, most AMPs are very hemolytic and toxic to mammalian cells (mellitin,[8] guavanin 2,[9] etc.), avoiding their use orally; therefore, only topical formulation is possible in the majority of cases (commercial triple antibiotics).[10]

The design of new and less toxic peptide drugs, for oral and systemic administration, is desired. Although there are many publications about AMPs as the antibiotics of the future, they do not have the expected impact yet. New roads must be accessed in order to improve this.[5]

In recent years, peptides have received increasing attention as pharmaceuticals despite their intrinsic drawbacks in terms of pharmacological properties. The attractiveness of peptides as drugs is mainly due to their high degree of specificity in comparison with conventional chemical drugs. Furthermore, massive peptide synthesis can be performed in a cost−benefit manner and more effective ADME (administration, distribution, metabolism, and excretion) parameters can be obtained with rationally designed peptide derivatives.[11]

Peptide drugs are quite common nowadays;[12] however, their usage is limited due to their low metabolic stability, oral absorption, rapid excretion through the kidney and liver, low immunogenicity, and high hemolytic activity.[13]

Cm-p5 (SRSELIVHQRLF-NH_2) is a peptide derived from a coastal tropical snail, *Cenchritis muricatus* (*Gastropoda: Littorinidae*), that showed antifungal activity against the human pathogens *Candida albicans*, *Candida parapsilosis*, *Cryptococcus neoformans*, *Trichophyton mentagrophytes*, and *Trichophyton rubrum*. This peptide did not exhibit any toxicity against a mammalian cell line in vitro and was structurally characterized by circular dichroism polarimetry and NMR spectroscopy,[14] revealing an α-helical structure under conditions that mimic a cellular environment and a tendency to a random structure in aqueous solutions.[15]

Cm-p5 is not a suitable therapeutic agent due to its easy proteolytic degradation. The presence of two Arg residues in the structure probably facilitates trypsin degradation, and the free *N*-terminal can be targeted by aminopeptidase action. The covalent modification of this peptide could improve its metabolic stability once the importance of each amino acid residue for its biological activity was dertermined.[12]

Cm-p5 showed a fungistatic action in the 10−40 μg/mL range against *Candida albicans*. This is a similar effect to that observed for the conventional antifungal fluconazole[16] but different than amphotericin B, which exhibited a fungicidal character, eliminating the microbial population in 24 h.[16]

In a plethora of cationic AMPs existing today, we selected Cm-p5 due to its low hemolytic and cytotoxic activity,[16] the simplicity of its synthesis and some covalent modification, and its similar antifungal activity compared to conventional fungistatics like fluconazole (MIC = 8−16 μg/mL, against *Candida albicans*).[17]

The biological mechanism of action of Cm-p5 is currently unknown. However, this molecule interacts preferentially with fungal phospholipids and does not interact with ergosterol (unlike amphotericin B), and to our knowledge, there is no information regarding whether it is present in the cytoplasm. Based on the previous aspects, four action mechanisms can be hypothesized: (i) destabilization of the cellular membrane,[18] (ii) inhibition of cell wall synthesis (like echinocandins),[19] (iii) inhibition of ergosterol synthesis[20] (like clotrimazole and fluconazole), and (iv) intracellular enzymatic inhibition.[21] In any case, helical stabilization of Cm-p5 may play an essential role in its biological activity.

In this article, we present a general study of the relevance of several amino acids in the biological activity of Cm-p5. This revealed the essential role of Glu and His residues in the helix stabilization and allowed us to synthesize a mutant by changing them for Cys. The mutant and the two unexpected dimers presented an improved antimicrobial activity and possibly enhanced pharmacological properties.

RESULTS AND DISCUSSION

Design of Mutants of Cm-p5. Normally alanine scanning is conducted for estimating the relative importance of each amino acid in the biological activity of peptides.[22] However, a simpler and faster approach is the rational change of amino acids[23] according to the natural structures currently found in AMPs, like the presence of many Arg, Lys, Cys, and Trp residues (His in the case of histatins),[24] and alternated positive charges to form a facial amphiphilic α-helix or β-sheet. This is a

DOI: 10.1021/acsomega.9b02201
ACS Omega XXXX, XXX, XXX−XXX

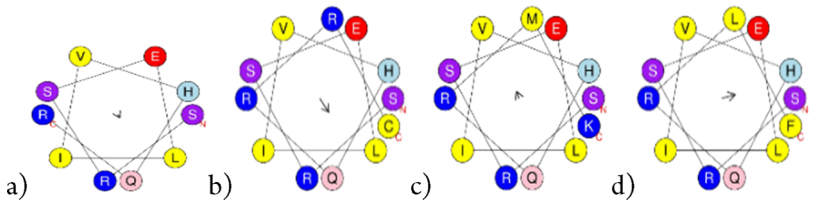

Figure 1. Schiffer–Edmundson projections of the antifungal peptides (a) Cm-p1, (b) Cm-p3, (c) Cm-p4, and (d) Cm-p5.

Table 1. Helical Parameters for Nonamidated Cm-p1, Cm-p3, Cm-p4, and Cm-p5[a]

peptide	helix	H	μHrel	z	FreqPolar	angleM
Cm-p1	SRSELIVHQR	0.18900	0.05685	1	0.700	5.18806
Cm-p3	SRSELIVHQR**RC**	0.20167	0.21172	2	0.667	5.35967
Cm-p4	SRSELIVHQR**MK**	0.17750	0.09499	2	0.667	1.98272
Cm-p5	SRSELIVHQR**LF**	0.44833	0.19215	1	0.583	0.24380

[a]H: hydrophobicity, μHrel: relative dipole moment of hydrophobicity, z: total charge, FreqPolar: frequency of polar groups, angleM: angle in radians between the horizontal plane and direction of μHrel.

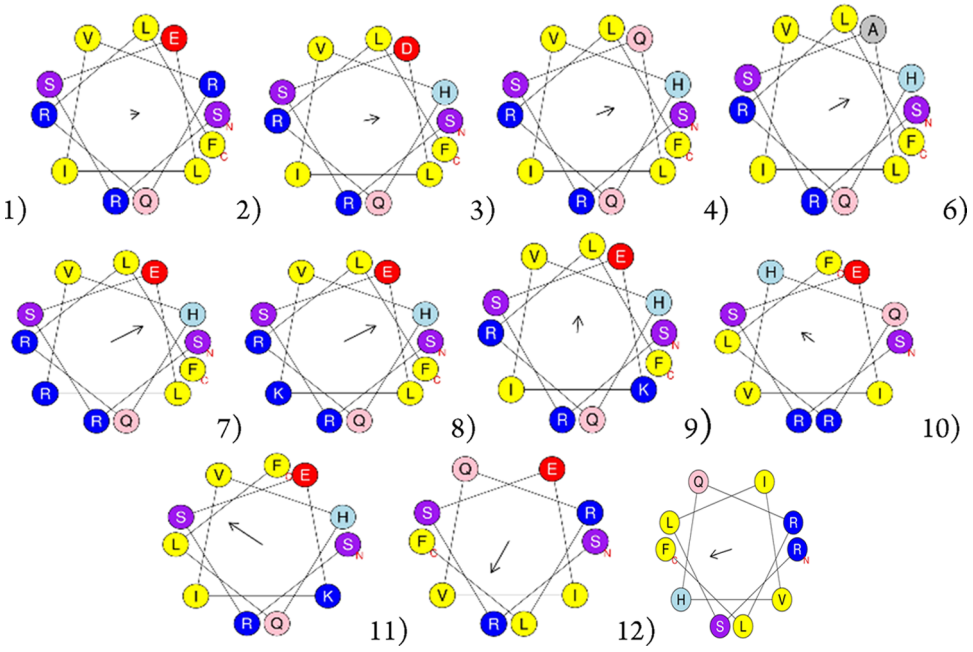

Figure 2. Schiffer–Edmundson projection of peptides analogues of Cm-p5.

fundamental structural principle that works well in many cases, possess a shape in which cationic and hydrophobic amino acids organize spatially in discreet sectors of the molecule, forming an amphipathic pattern.[25]

Tryptophan is frequently found in interaction with the interfacial region of the lipid membrane;[26] Arg and Lys have positive charges at physiological pH, permitting the selective interaction with microbial membranes; and Cys, in certain conditions, stabilizes secondary structures by forming disulfide bridges.[27]

Based on a simple electrostatic interaction model between cationic AMPs and negatively charged bacterial/fungal membranes, several specific structural features in the helix projection of Cm-p5 are notable. This peptide presents hydrophobic residues at the C-terminus, a free N-terminus (positively charged), and an amphipathic helical structure with positive charges concentrated toward one side of the helix but a less defined hydrophobic region.

Analyzing the Schiffer–Edmundson projection of Cm-p5 (Figure 1d), it is possible that the polar side of the helix contains an unexpected hydrophobic Ile residue. In addition, polar residues, such as Glu and His, are curiously present in the putative hydrophobic face.

Previous research[13] has demonstrated that inserting Arg-Cys (forming Cm-p3) or Met-Lys (forming Cm-p4) in the C-terminus of the mollusk-derived peptide Cm-p1 did not improve the antimicrobial activity; however, Leu-Phe (forming Cm-p5) insertion furnishes a high antifungal activity (Figure 1).

Using the online server http://heliquest.ipmc.cnrs.fr/cgi-bin/ComputParams.py, helical parameters[28] of helicoidal peptides were obtained. Hydrophobicity (H; intrinsic capability of a peptide to move from an aqueous into a hydrophobic phase), frequency of polar residues (Freq. Polar), relative hydrophobic moment (μHrel; quantitative measure of peptide amphipathicity[29] defined as the vector sum of the hydrophobicities of the individual amino acids), and the angle moment (angleM; angle

DOI: 10.1021/acsomega.9b02201
ACS Omega XXXX, XXX, XXX−XXX

Table 2. Helical Parameters of Cm-p5 Analogues

peptide	helix	H	μHrel	z	FreqPolar	angleM
Cm-p5	SRSELIVHQRLF	0.44833	0.19215	1	0.583	0.24380
Change of His						
1	SRSELIV**R**QRLF	0.35333	0.09818	2	0.583	0.14196
Change of Glu						
2	SRS**D**LIVHQRLF	0.43750	0.18479	1	0.583	0.20159
3	SRS**Q**LIVHQRLF	0.48333	0.21791	2	0.583	0.35966
4	SRS**A**LIVHQRLF	0.52750	0.25359	2	0.500	0.47042
5	SRS***β*****A**LIVHQRLF					
Change of Ile						
6	SRSEL**R**VHQRLF	0.21417	0.41547	2	0.667	0.49375
7	SRSEL**K**VHQRLF	0.21583	0.41384	2	0.667	0.49293
Change of Leu						
8	SRSE**K**IVHQRLF	0.22417	0.19104	2	0.667	1.49355
Truncated and change of Leu by Lys						
9	SRSE-IVHQRLF	0.33455	0.18199	1	0.636	2.44770
10	SRSE**K**IVHQ-LF	0.33636	0.46847	1	0.636	2.52341
11	-RS-LIVHQRLF	0.6060	0.33231	2	0.500	3.41529
12	SRSE-IV-QRLF	0.35500	0.42451	1	0.600	4.21201
Additional variants						
13	**Ac**-SRSELIVHQRLF					
14	$(SRSELIVHQRLF)_2K$					

Table 3. Biological Activity Measured as Minimal Inhibitory Concentration (MIC) against Different Bacteria and Fungi for Each Synthesized Peptide[a]

		MIC (μg/mL)				
no.	peptide	Sa	Ec	Ca	Cp	Tr
1	SRSELIV**R**QRLF-NH_2	>400	>400	>400	>400	>400
2	SRS**D**LIVHQRLF-NH_2	>400	>400	>400	>400	>400
3	SRS**Q**LIVHQRLF-NH_2	>400	>400	>400	>400	>400
4	SRS**A**LIVHQRLF-NH_2	>400	>400	>400	>400	>400
5	SRS***β*****A**LIVHQRLF-NH_2	>400	>400	>400	>400	>400
6	SRSEL**R**VHQRLF-NH_2	NT	NT	>400	>400	NT
7	SRSEL**K**VHQRLF-NH_2	NT	NT	>400	>400	NT
8	SRSE**K**IVHQRLF-NH_2	>400	>400	>400	>400	>400
9	SRSE--IVHQRLF-NH_2	>400	>400	>400	>400	>400
10	SRSE**K**IVHQ--LF-NH_2	>400	>400	>400	>400	>400
11	-RS--LIVHQRLF-NH_2	>400	>400	>400	>400	>400
12	SRSE--IV--QRLF-NH_2	>400	>400	>400	>400	>400
13	**Ac**-SRSELIVHQRLF-NH_2	NT	NT	10	10	10
14	$(SRSELIVHQRLF)_2K$-NH_2	NT	NT	>400	>400	NT
	ampicillin	0.02	0.1953	NT	NT	NT
	amphotericin B	NT	NT	0.25	0.25	0.125

[a]Ca = *Candida albicans*, Cp = *Candida parapsilosis*, Tr = *Trichophyton rubrum*, Sa = *Staphylococcus aureus*, Ec = *Escherichia coli*; NT = not tested.

in radians between the horizontal plane and direction of μHrel) are listed in Table 1.[30]

All calculations were realized supposing the α-helical structure and as an explication of the loss of antifungal activity for all these analogues of Cm-p5.

When analyzing the effect of these C-terminal modifications in the Cm-p1 activity in detail, we observed that the addition of Arg-Cys (forming Cm-p3) does not change the frequency of polar groups considerably, hydrophobicity, or orientation (arrow in Figure 1b) of the relative hydrophobic moment but significantly alters the μHrel magnitude (Table 1). In contrast, the insertion of Met-Lys (forming Cm-p4) turns the direction of μHrel (arrow in Figure 1c) but poorly increases its magnitude (Table 1). Addition of Leu-Phe (forming Cm-p5) greatly modifies all parameters, especially H and μHrel (arrow in Figure 1d and Table 1). In this case, Phe is located in a *i*,*i*+4 position in relation to His; therefore, there may occur a π−π interaction between the phenyl and imidazole groups of these residues, which could have some effect in helix stabilization. Based on a previous article,[15] Cm-p4 is a more active version of Cm-p1 than Cm-p3, which may indicate that the variation of the direction of μHrel is more relevant than the variation of its magnitude, particularly in Cm-p5, where μHrel is almost directed from the hydrophilic to the hydrophobic face (arrow in Figure 1d).

These previous results apparently suggest that magnitudes of H, μHrel, or its direction are fundamental for activity, favoring sequences with elevated H (intrinsic capability of a peptide to move from an aqueous into a hydrophobic phase) or μHrel (quantitative measure of peptide amphipathicity) and direction

DOI: 10.1021/acsomega.9b02201
ACS Omega XXXX, XXX, XXX−XXX

of μHrel from the hydrophobic to hydrophilic phase to promote membrane interaction.

Considering these suggestions, 14 analogues of Cm-p5 (Figure 2 and Tables 2 and 3) were designed based on SAR (structure−activity relationship). The experimental strategy of this work, with a minimal use of resources, was to gain an insight into how the antifungal activity of the Cm-p5 is affected by the change of amino acid sequence. Arg residues remained in almost all cases since positive charges are supposed to be likely in the polar face of the helix and are essential for membrane interaction and biological activity.

The fundamental modifications introduced in the sequence of Cm-p5, based on amino acid charge at physiological pH were as follows: (i) change of the negative Glu residue, (ii) introduction of another positive charge by mutation of Lys or Arg by Ile, (iii) change of His by a positively charged Arg, (iv) change of Leu5 by another positively charged residue (Lys), and (v) truncated versions, where residues such as Leu, Arg, Ser, Glu, or His were eliminated.

All the performed changes will assist in evaluating the contribution of each mutated residue to the helical stabilization and therefore to the biological activity of the peptide. Glu was modified by the similar but neutral Gln (peptide 3 in Table 2); in the case of Asp (peptide 2 in Table 2), the negative charge was maintained but the length of the lateral chain was modified. The charge was also eliminated by the mutations of Ala (peptide 4 in Table 2) and β-Ala (peptide 5 in Table 2), simulating the classical alanine scanning. Changing His for Arg (peptide 1 in Table 2), we will assess the role of the neutral His residue at physiological pH and the effect of a permanent positive charge. Further changes like Ile for Lys (peptide 7 in Table 2) or Arg (peptide 6 in Table 2) will introduce another positive charge within the hydrophilic face. Truncated analogues could indicate, for example, if the activity is influenced by the interaction of Glu and His in i+3 (peptide 9 in Table 2) or Glu and Lys in i+2 (peptide 10 in Table 2).

Dimeric MAP (multiple antigenic peptides)-type peptide was synthesized since activity improvement in these cases was reported.[31] N-terminal acetylated Cm-p5 was produced to evaluate if the positively charged free N-terminus contributes to the antifungal activity.

Chemical synthesis is a valuable tool to obtain analogues of biologically active peptides found in natural sources. The experimental feasibility of SPPS (solid phase peptide synthesis) allowed us to introduce rational changes to the peptide sequence in order to generate several diverse structures. Fmoc/tBu chemistry is preferred and more useful if the peptides do not aggregate. Rink-MBHA-Resin is useful for the production of amidated peptides, and a first-generation polystyrene support is adequate for short sequences.

Results and Discussion regarding Cm-p5 Peptide Mutants. Fourteen peptides were synthesized based on the previous design (Table 2). C-terminals of all the peptides were amidated (−NH2) since an Fmoc-Rink-MBHA resin was used. The Rink linker and the side-chain protecting groups, as expected, resulted in a stable (orthogonal) functional group toward Fmoc elimination treatment (piperidine 20% in DMF) and coupling conditions. DIC/Oxyma combination (less than 1% of racemization) was used for each manual coupling, showing an excellent efficiency due to the simplicity of synthetized sequences. Final cleavage and side-chain deprotection, ether precipitation, centrifugation, and lyophilization produced the crude product, ready for analytical mass determination and the purification process.

Functional screening of the designed peptides based on antibacterial and antifungal activities are listed in Table 3. Amphotericin B and ampicillin were used as controls for fungal and bacterial strains, respectively.

To our surprise, no amino acid changes maintain or improve the antimicrobial activity of Cm-p5, indicating an essential sequence characteristic needed to exert the biological activity.

Substitution of His by Arg (peptide 1 in Table 2) involved a change in the protonation state of the amino acid in position eight, increasing the lateral chain length (reduce distance to the negative Glu), μHrel decreases to half, and its direction changed slightly with respect to Cm-p5 (Table 2 and Figure 2). Decrement of μHrel, change in the length of the lateral chain, and/or the presence of permanent positive charge at the His position is not good for the activity.

Similarly, modification of Glu residue to either Gln, Ala, βAla, or Asp (peptides 2−5 in Table 2) resulted in the loss of antimicrobial activity. Apparently, the negative charge in the Glu residue (changing Glu by Gln) and the distance to that (changing Glu by Asp) are essential for the activity, even more if we consider that the magnitude of μHrel and values of Hare practically the same when Gln or Asp is present instead of Glu. Modification to Ala (peptide 4 in Table 2), as expected, alters the H and magnitude of μHrel but especially its direction, indicating some additional effects. β-Ala (peptide 5 in Table 2) has a similar behavior.

In order to increase the amphipathicity, we added a positive residue (Arg or Lys) in the hydrophilic face instead of Ile. In these cases, the change in the direction of μHrel is higher (augmented angle between the horizontal plane and direction of μHrel), compared to any previous analogue, while H is half, but μHrel doubles (as expected, increase the amphipathicity). However, the original Arg apparently generates such repulsion with the additional Arg or Lys (peptides 6 and 7 in Table 2) residues located in the same face, which may destroy the helical conformation.

Peptide 8 in Table 2 was also inactive. In this, the change of Leu5 by Lys produces a major increase in the angle between the horizontal plane and the μHrel, but its magnitude is maintained and H is reduced by half. In addition, unfavorable electrostatic interaction between Glu and Lys residues could be implicated in the inactivation of this analogue.

The behavior of truncated versions of Cm-p5 in terms of biological activity was mostly random and more difficult to understand, but remarkably, all these peptides change the direction of μHrel dramatically when compared with Cm-p5.

The direction of μHrel can be more important for the correct interaction with the membranes than its magnitude (amphipathicity), considering that during Arg contact with a negative phospholipid, only the vertical component of this vector, which splits in half the helix from Arg to the opposed face (helix axis), is in cooperation with the dipole moment vector of the membrane.

If the μHrel direction has more horizontal components (perpendicular to the axis of the helix), then its real magnitude is neglected, and repulsive forces are implicated in an augmented instability of the peptide bounded to the membrane system even if positively charged residues, concentrated in one face, are present (Figure S1a, Supporting Information).

Acetylated Cm-p5 maintains fungistatic properties (peptide 13 in Table 2); therefore, free N-terminal is not needed for

DOI: 10.1021/acsomega.9b02201
ACS Omega XXXX, XXX, XXX−XXX

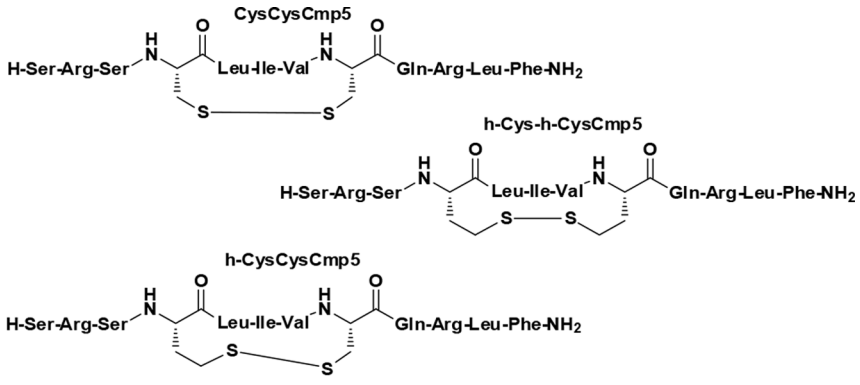

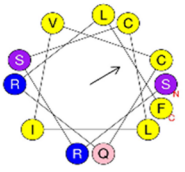

Peptide	H	μHrel	z	F. Polar	angleM
CysCysCm-p5	0.7475	0.45805	2	0.417	0.56152
Cm-p5	0.4483	0.19215	1	0.583	0.24380

Figure 3. Designed cyclic analogues of Cm-p5, helical wheel projection of CysCys-Cm-p5, and helical parameters.

activity, enabling the total protection of peptide toward aminopeptidase degradation in future research.

The dimeric version (peptide 14 in Table 2), like MAP (multiple antigenic peptides), did not show any activity. This may be due to steric hindrance between C-terminal joined chains, which would imply helix destruction.

In general, our results suggest four determinant structure factors in order to maintain the biological activity of Cm-p5. Glu and His residues must be in the *i*,*i*+4 positions, μHrel vector must be close to a parallel direction with respect to the membrane pointing in the opposite direction of the hydrophilic face (Arg residues), and any repulsive interaction that could interfere in helicity should be avoided.

Salt Bridge and Helical Stabilization. Based on the previous modifications (Table 3), we consider that the most remarkable finding was the relative position of His and Glu (pK_{aR} = 4.25, α dissociation grade = 99.97%) (analytical calculation based on a concentration of 10 μg/mL of Cm-p5 and physiological pH = 7.4) in Cm-p5. These residues could be participating in helical stabilization by forming salt bridges (defined as the combination of two noncovalent interactions: electrostatic interaction and hydrogen bonding).[32] For Cm-p5, the modification of these residues (peptides 1−5 in Table 2) or the distance between them (peptide 9 in Table 2) involves the loss in biological activity. Recently, the role of salt bridge interaction in secondary structure stabilization of single α-helix of peptides has been revealed.[33]

In proteins, such as T4 lysozyme, a salt bridge was identified between Asp (pK_{aR} = 3.65, α = 99.93%, supposing 10 μg/mL) at residue 70 and a His at 31. Although the imidazole ring of His31 is not protonated at physiological pH (pK_{aR} = 6.8, α = 79.85%, supposing 10 μg/mL), it demonstrated a shift in its pK_{aR} (protonated imidazole) to 9.05 (α = 2.19% at 10 μg/mL) in the folded protein that simulates a protonated His at pH = 7.4 due to salt bridge formation.[34]

Cm-p5 changes to a helical conformation only by interacting with membranes. In internal protein media or under membranolytic conditions, water content is low,[35] solvation of negative Asp or the imidazole ring is not effective, and the salt bridge can be formed spontaneously by negative enthalpy and entropy (hydrophobic effect). A possible mechanism, by which this process could take place, is the formation of a hydrogen bond between the neutral imidazole (pK_{aR} = 13.1)[36] and the negatively charged Asp residue. This donation of negative charge by Asp to the imidazole ring increases its basicity, in consequence the pK_{bR} (from 7.2 to 4.95) (pK_{aR}: from 6.8 to 9.05) and its protonation grade from 20.25 to 97.81%.[34] In principle, the hydrolysis pK_{hR} = pK_{bR} of imidazole decrease (pK_{aR} increases) because of the effect of the negative charge of Asp at pH = 7.4 (Figure S1b, Supporting Information). Weak acids or anions such as phosphate, water solvation, or monopositive cations (Na^+ or K^+) do not favor salt bridge formation (Figure S1c, Supporting Information). On the other hand, di-positive cations (Ca^{2+} or Mg^{2+}, perform as counter ions of phosphate in membranes) could reinforce the interaction (Figure S1d, Supporting Information). This is the first time that a salt bridge between His and Glu in the *i*,*i*+4 position is proposed and further investigation is needed to confirm its role in helical stabilization and, consequently, in the biological activity of Cm-p5.

If this salt bridge is essential for the antifungal activity of Cm-p5, in environments such as mucosa, skin, or tumors, where pH = 5−6, then the biological effect will be enhanced due to alteration in the dissociation grade of Glu (85% at pH = 5) or protonation grade of His (96.89% at pH = 5). Also, the influence of the ionic strength or type of ions may alter these noncovalent interactions.[24,31] We assumed that covalent cyclization between these residues by substituting them with Cys should stabilize the helical secondary structure, energetically favoring the action mechanism. A disulfide bridge (or any other covalent stabilization) should overcome all drawbacks related with the physiological behavior of this salt bridge and make peptides more resistant to proteolysis.

It is currently known that cyclization in *i*,*i*+3 or *i*,*i*+4 positions can stabilize an α-helix.[37] In order to know whether Cys residue has the suitable length for maintaining a helical conformation without further deformation, we made a molecular dynamic study of mutated Cm-p5 (E4C and H8C) to estimate the covalent distance between thiol groups in the *i*,*i*+4 position. Analysis of the distance between sulfur nuclei shows that they

DOI: 10.1021/acsomega.9b02201
ACS Omega XXXX, XXX, XXX−XXX

Scheme 1. Synthesis of Disulfide-Bridged Analogues of Cm-p5

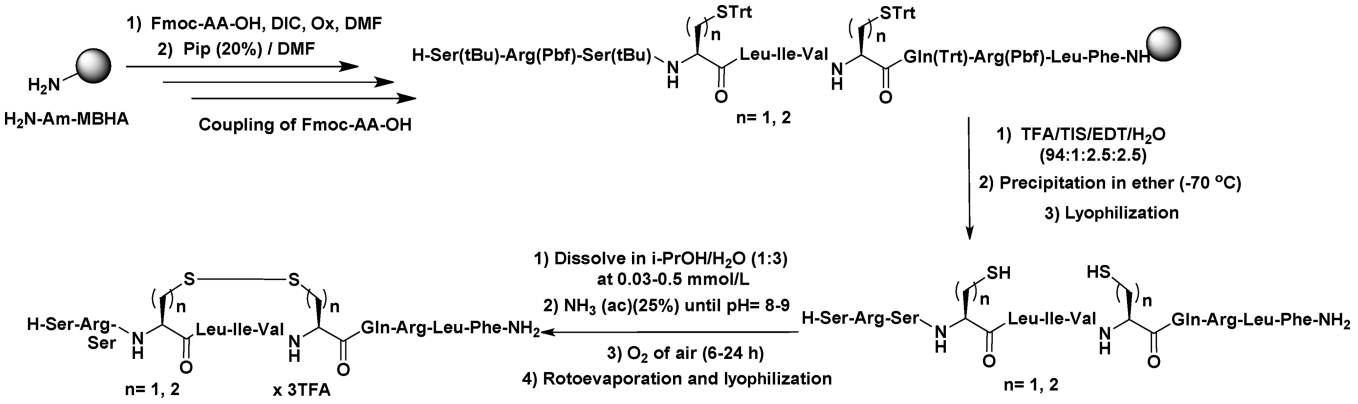

Scheme 2. Synthesis of CysCysCm-p5 Parallel Dimer Using the Orthogonality between Acm and Trt Protecting Groups

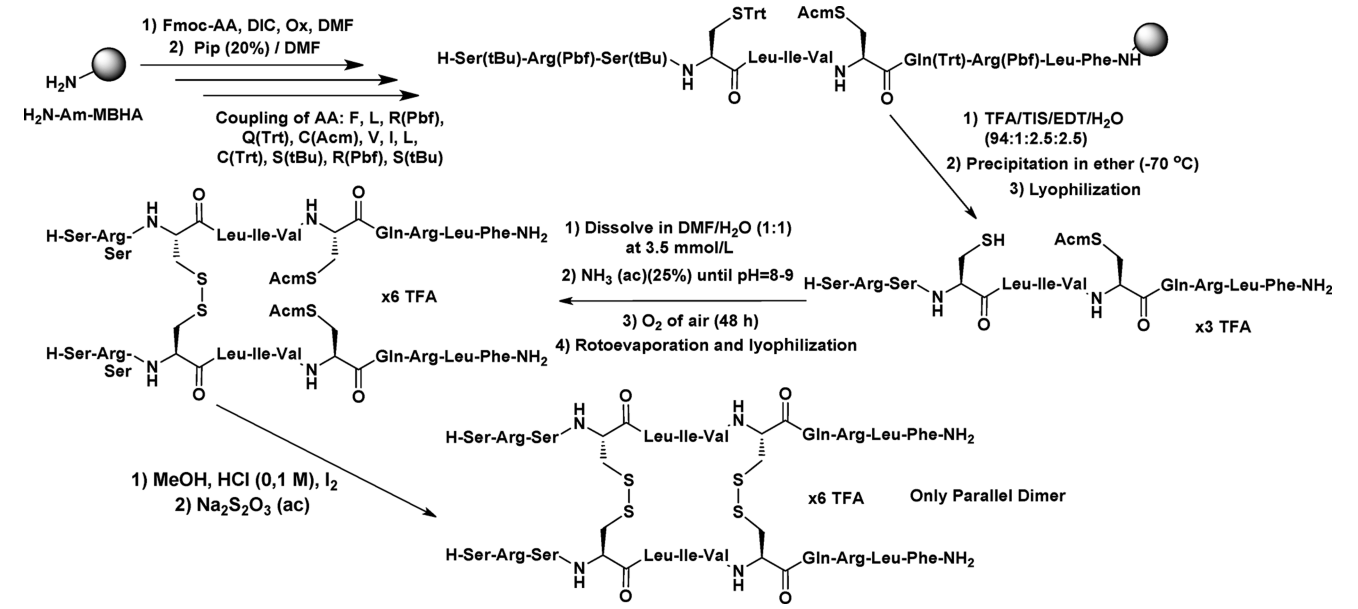

are located on the edge (2−10 Å) of the sulfur covalent radius (1.05 Å) This result also shows that using homo-cysteine (Hcy) residues or a combination of Cys and Hcy could improve the cyclization process and, consequently, helical stabilization.

With this aim in mind, we synthesized three new peptides, placing two Cys, two Hcy or one Cys, and one Hcy instead of the Glu and His pair (Figure 3). It is important to note that, like in Cm-p5, these analogues have doubled the H value, μHrel magnitudes, and its direction totally opposed to Arg residues, without any horizontal component that can repel the membrane relative dipole moment (Figure 3).

Results and Discussion regarding Salt Bridge and Helical Stabilization. The synthetic procedure for Cm-p5 cyclic analogues is presented in Scheme 1. Following the Fmoc/*t*-Bu peptide strategy, cleavage in the presence of EDT, three new acyclic analogues were produced with high purity and yield (Scheme 2).

The three di-thiolated peptides were submitted to the cyclization process by means of in-water oxidations with air oxygen, showing some specificity for each compound. Usually, in similar transformations with other peptides, all acyclic starting materials are consumed in 2−3 h. In the case of the CysCysCm-p5 analogue, more time (6 h) was needed for the consumption of all starting materials, and coincidently, acyclic and cyclic monomers have the same retention time; therefore, only mass analysis or Elman test could confirm the total conversion (Figures S17 and S18, Supporting Information). In a first attempt, desulfured impurity was produced due to increased pH (above 9). However, this problem was corrected by maintaining the pH strictly around 8−8.5. Surprisingly, in the standard cyclization conditions used for commercial peptides in our laboratory (0.5 mM), the CysCysCm-p5 analogue produced considerable quantities of dimeric byproduct (Figures S17 and S18, Supporting Information), considered as parallel and antiparallel dimers (Figure 4). Similar dimers were reported as

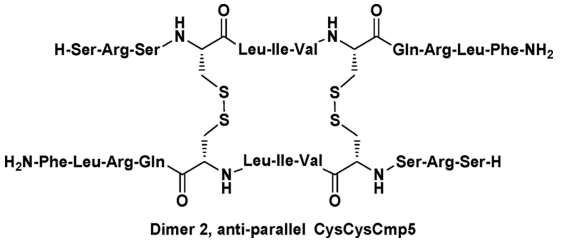

Figure 4. Antiparallel dimeric CysCysCm-p5.

DOI: 10.1021/acsomega.9b02201
ACS Omega XXXX, XXX, XXX−XXX

Chart 1. CD Analysis in Water and 10% SDS[a]

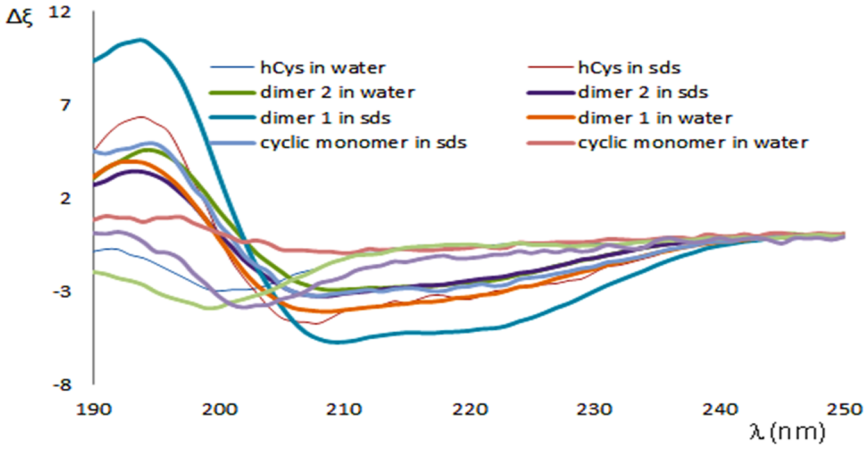

%	hCys $_{w}$	hCys $_{sds}$	Cm-p5 $_{w}$	Cm-p5 $_{sds}$	Cyclic $_{w}$	Cyclic $_{sds}$	Dimer 1 $_{w}$	Dimer 1 $_{sds}$	Dimer 2 $_{w}$	Dimer 2 $_{sds}$
Helix:	4,2	25,9	4	7,6	1,5	24,8	24,7	49,6	23,5	23,7
Antiparallel:	27	8,1	26,3	24,1	41,9	14,5	7,7	2	17,4	22,9
Parallel:	1,6	0,8	5,7	0.0	0	0,8	6,1	0	2,1	0,4
Turn:	17	13,2	16,5	16.6	13	14	13,1	9,2	13,4	11,5
Others:	50,2	52,1	47,6	51,7	43,6	45,9	48,4	39,3	43,6	41,5

[a]Secondary structure content (in percentage) calculated with the online program Bestsel (http://bestsel.elte.hu). hCys: cyclic HcyHcyCm-p5, Cyclic: cyclic CysCysCm-p5, Dimer 1: parallel dimer, Dimer 2: antiparallel dimer.

impurities of CIGB-300 anticancer peptide.[38] Peak 4 (Figure S17, Supporting Information) represents a conformer of peak 3, a dimer, as can be seen in the ESI-HRMS spectrum (Figure S18, Supporting Information) and due to coalescence between peaks 3 and 4 if the sample is previously stabilized for 2 h at room temperature.

Only at 0.03 mM the production of the cyclic monomer without the formation of dimeric byproducts (Figure S21, Supporting Information) is guaranteed. However, this concentration is not actually applicable to industrial processes, and a better strategy would be to perform the cyclization on resin and final cleavage of the cyclic monomer as a crude product.

In order to identify which peak in the RP-HPLC corresponds to the parallel or antiparallel dimer, we decided to change the orthogonality of Cys protection, using Cys(Acm) for the His mutation and Cys(Trt) for the Glu. With these new protecting groups, peptide cleavage from resin produced an acyclic monomer containing Cys(Acm) and a free Cys residue. Dimerization of this compound at concentrated conditions (5 mM) (Figure S23, Supporting Information), solvent evaporation, lyophilization, and finally Acm deprotection with iodine and further cyclization guaranteed the production of the parallel dimer only. This unequivocal parallel dimer has the same retention time compared to the first dimer produced in the CysCysCm-p5 peptide cyclization (Figure S24, Supporting Information), confirming the identification of the parallel dimer and the antiparallel counterpart.

As a comparison, cyclization of the peptide containing both Cys and Hcy has less tendency to form both dimeric products under the same conditions (Figures S26 and S27, Supporting Information). In the case of the analogue with two Hcy, only the cyclic monomer is obtained at 0.5 mM (Figure S30, Supporting Information).

In conclusion, intrachain disulfide bridge between *i*,*i*+4 (residues 4 and 8) positions in Cm-p5 are more feasibly accessible when two Hcy or Hcy-Cys combinations are introduced. On the contrary, inter-chain disulfide bridge when Cys-Cys combination is introduced are clearly limited by steric hindrance. This type of inter-chain disulfide bridge is similar to the ones that are present in insulin and defensins. However, this is the first report, to our knowledge, of disulfide dimers between *i*,*i*+4 positions.

Circular Dichroism Analysis. The following peptides were submitted to CD analysis in water and 10% SDS−water mixture: Cm-p5 (CysCysCm-p5 cyclic monomer), HcyHcyCm-p5 (cyclic monomer), and the parallel and antiparallel dimers of CysCysCm-p5. It is evident that a better helical stabilization was obtained for the cyclic monomers in a 10% SDS solution when compared with Cm-p5 (Chart 1). At 10% SDS (micellar critic concentration of SDS) and despite the difference in surface curvature, these types of micelles are similar or mimic biological membranes of bacteria and fungus and are also negatively charged. Remarkably, in the case of dimeric compounds (Chart 1), interaction with micelles is not needed for helicity induction; these compounds are predominantly α-helices in water.

Interestingly, the CysCysCm-p5 cyclic monomer showed a major percentage of antiparallel β-structures in water than in the case of HcyHcyCm-p5. It is important to note that dimer 1 (parallel) does not show an antiparallel β-strand structure under aqueous or SDS conditions if compared to dimer 2 (antiparallel). Also, the latter has the same behavior in water or SDS, which may be an indication of the double repulsion between the free positive *N*-terminal (with hydrophilic interactions) and the hydrophobic Leu-Phe at the C-terminus (with hydrophobic interactions) for this antiparallel construction (acetylated version of CysCysCm-p5 could totally avoid this drawback). Based on the results shown in Chart 1, it is possible to conclude that, for the dimers, the interchain disulfide bridge is responsible for maintaining 25% of the helical structure in water. Only in the case of the parallel dimer (dimer 1) water molecules are excluded by SDS, and additionally, hydrophilic and hydrophobic interactions at the N- and C-terminal contribute to considerably increase (up to 49%) the total segment of the helix (Chart 1).

DOI: 10.1021/acsomega.9b02201
ACS Omega XXXX, XXX, XXX−XXX

Molecular Dynamic Study of Helical Stabilization. Molecular dynamic simulations of the CysCysCm-p5 dimers and monomers were performed with the aim to determine helical stabilization in different solvents. It is known that TFE is a membranolytic solvent capable of inducing helical structures in peptides. Our idea was to find a behavior similar to CD analysis in which we could demonstrate that a disulfide bridge in the *i*,*i*+4 position of Cm-p5 stabilizes the helical structure in water or TFE/water (40%) mixtures. Simulations were performed using a helix as the initial structure and evolution was followed over 50 ns (Table 4).

Table 4. Composition of the Simulated Systems and α-Helix or Turn Content (%) Calculated during the Last 10 Ns (of the Total 50 ns)

simulated systems[a]	SPC[b]/TFE	NCI[c]	α-Helix[d]	turn	coil	others
Cm-p5$_w$	1886/0	−2	53 (75)	8	33	5
Cm-p5$_{mix}$	1302/126	−2	71 (75)	3	25	1
CysCysCm-p5$_w$	2078/0	−3	37 (75)	15	39	9
CysCysCm-p5$_{mix}$	1433/139	−3	61(75)	13	19	7
parallel dimer$_w$	3022/0	−6	74 (72)	1	21	4
parallel dimer$_{mix}$	1556/253	−6	68 (72)	3	25	4
antiparallel dimer$_w$	3515/0	−6	74 (72)	1	20	4
antiparallel dimer$_{mix}$	1856/267	−6	60 (72)	2	34	4

[a]w: water and mix: TFE/water. [b]SPC: simple point charge (water model used). [c]NCI: number of counter ions (Cl^-); the sign indicates the charge of the ion. [d]Initial α-helix structure content is reported in parentheses.

In Figure 5A, the total helix length (a typical helix property) for the native Cm-p5 peptide in both pure water and TFE/water mixture as a function of time is reported. It is evident that this peptide maintains a stable helix structure in the TFE/water mixture during the whole simulation, in contrast to that in pure water. Furthermore, according to the secondary structure analysis, based on the Dictionary of Secondary Structure of Proteins criteria, this peptide is defined as a 53% α-helix in water and 71% in TFE/water (Table 4). This type of behavior is common to helical peptides in membrane-mimetic conditions.[15,39] The effect of TFE on peptides has been reported previously, where TFE excludes water by aggregating around the peptide, favoring the formation of intramolecular hydrogen bonds and promoting the formation of a secondary structure.[40] Of note, the CysCysCm-p5 monomer has 15% of turn in the last 10 ns, indicating the tendency of this to form both helical structure and β-structure (Table 4).

We also constructed a mutated parallel dimer of Cm-p5 to evaluate its behavior in pure water and TFE/water mixture. This biomolecule manifests a higher tendency to the helical structure in water (Chart 1). The fact that this molecule maintains its helicity in water can be visualized through MD (molecular dynamic) simulations. In Figure 5B, it is clear that this peptide maintains a stable helix structure in both solvents. In fact, it behaves in a similar fashion when placed in water compared to the native peptide in TFE/water according to the RMSF pattern (Figure 5C) and α-helix percentage (Table 4). In this case, a large deviation occurs for the charged N-terminus (Figure 5C) due to its favorable interaction with water molecules and that it possesses a high degree of freedom. An N-acetylated modification would be suited to decrease the N-terminus from fraying.

Overall, the parallel dimer is stable in water, conserving its characteristic α-helix (Table 4 and Figure 5B). This may be

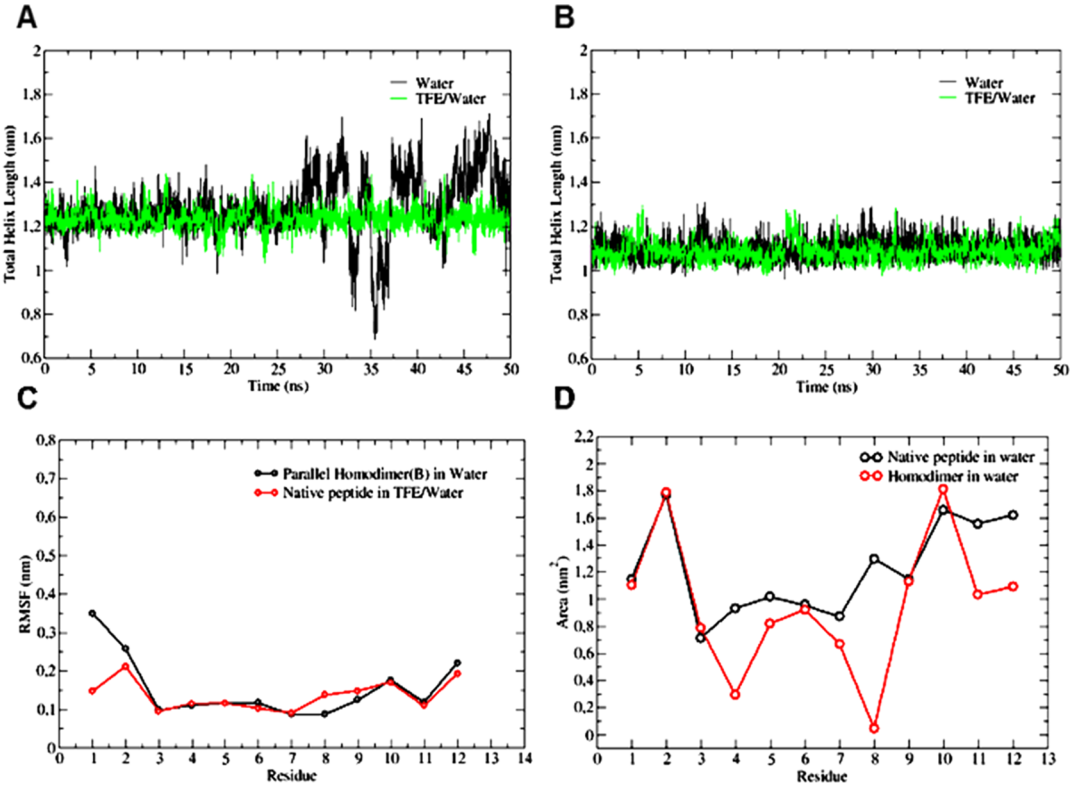

Figure 5. Total helix length (nm) over time (ns) of (A) native peptide and (B) one chain from the parallel dimer. (C) RMSF of each residue from one chain of the parallel dimer. (D) Solvent accessible surface area per residue over the last 10 ns of the trajectory.

DOI: 10.1021/acsomega.9b02201
ACS Omega XXXX, XXX, XXX−XXX

because of the decrease in solvent accessible area of nonpolar residues (Cys4, Cys8, Leu5, Val7, Leu11, and Phe12), which can be embedded between the monomers shielding them from water molecules and exposing polar residues (Ser1, Arg2, and Arg10) to the solvent (Figure 5D). The effect that one monomer has over the other could be similar to that of TFE when excluding water molecules (hydrophobic effect). Similar helical packing is present in globins or insulin, in which, as predicted by these parallel dimers, the angle between helix is 52°.[41] The angles between helix[42] in the parallel and antiparallel dimer were predicted as approximately 68° and 59° in the last 25 ns in water, respectively. The behavior of the antiparallel dimer was similar to the parallel dimer and is in accord with the ridges and grooves model of helix packing. Furthermore, our molecular dynamic simulations suggest that the antiparallel dimer helix is less stable than the parallel in the TFE/water mixture, and as shown in the CD experiment, dimer 2 has the same helical character in water or SDS (Chart 1), another indication that this compound is the antiparallel dimer.

In Vitro Anticandidal and Antibacterial Activity of cm-p5 and Its Derivatives. Antifungal activity was evaluated for Cm-p5, Hcy and Cys cyclic monomers (HcyHcy-Cm-p5 and CysCysCm-p5, respectively), and the two dimers (dimer 1 (parallel) and dimer 2 (antiparallel)) against three fungal and two bacterial species of clinical relevance (Table 5).

Table 5. Minimal Inhibitory Concentration (MIC) (μg/mL) of Cm-p5 and Its Derivatives against Three Candida and Gram-Positive and Gram-Negative Bacterial Species[a]

sample	Cm-p5	cyclic	dimer 1	dimer 2	Hcy
Candida species					
C. auris	11	27	30	31	NT
C. parapsilosis	32	14	39	>100	10
C. albicans	10	5	48	29	10
Bacterial species					
Listeria monocytogenes	>100	100	50	12.5	NT
Pseudomonas aeruginosa	>100	>100	>100	>100	NT

[a]Cyclic: cyclic CysCysCm-p5, Dimer 1: parallel dimer, Dimer 2: antiparallel dimer, Hcy: cyclic HcyHcyCm-p5.

The antifungal Cm-p5 peptide kept its expected anticandidal activity against *C. albicans* and *C. parapsilosis*, as previously described.[15] Interestingly, a relevant activity was also observed in the case of *C. auris*, an emerging nosocomial pathogen. The Hcy-Hcy cyclic monomer not only maintained the activity against *C. albicans* but also increased it against *C. parapsilosis*. The Cys cyclic monomer, even though it was not so effective against *C. auris*, it was able to decrease the MIC value against *Candida albicans*. The two dimers were the least effective against *Candida* species, showing MIC values around 30 μg/mL or even higher (Table 5).

To assess if these antifungal peptides also exert antibacterial activity, Cm-p5, the Cys cyclic monomer, and the two dimers were also analyzed in an agar diffusion assay (Table S1, Supporting Information) and by determination of the minimal inhibitory concentration (MIC). Table 5 shows the antibacterial MIC of Cm-p5 and its derivatives against the Gram-positive species *Listeria monocytogenes* and the Gram-negative species *Pseudomonas aeruginosa* confirmed the increased antibacterial activity of Cm-p5 dimers against *Listeria monocytogenes*. Cm-p5 exhibited a moderate antibacterial activity against *L. monocytogenes* at 1000 and 100 mg/L but had only minor effects against *P. aeruginosa* (Table S1, Supporting Information) at 1000 mg/L. The activity increased for the cyclic monomer and was highest for the two dimers, which showed a significant activity at 20 mg/L (Table S1, Supporting Information).

In Vitro Toxicity of Cm-p5 Analogues against Human Cells. Cytotoxicity of the cyclic monomer and the two dimers of Cm-p5 against macrophages and THP-1 human cells were also tested. At 300 μg/mL of each compound (a higher concentration than the one used to determine MIC against fungal or bacterial species), no toxicity effects were observed in terms of cell viability (Chart 2).

Chart 2. In Vitro Cytotoxicity of CysCysCm-p5 Cyclic Monomer and Dimers against Macrophages and THP-1 Human Cells

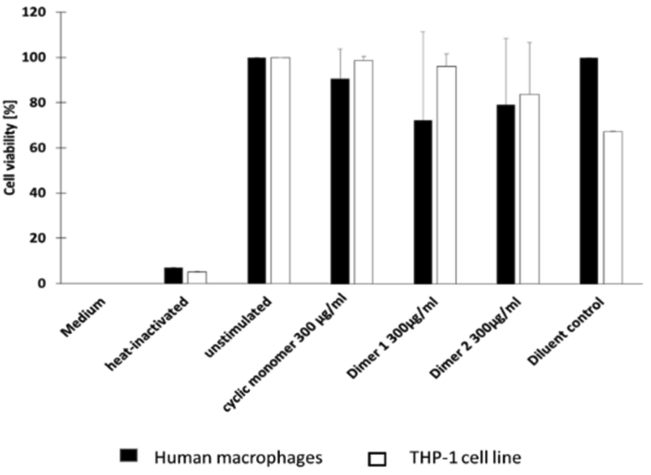

Discussion regarding Biological Activity. The cyclic monomer derived from the Cm-p5 antifungal peptide by an intrachain disulfide bond improved its anticandidal activity against *C. albicans* down to 5 μg/mL compared to the native Cm-p5 peptide (MIC = 10 μg/mL).[15] A similar improvement was observed against *C. parapsilosis* (from 32 to 14 μg/mL), and a decreased activity was observed against *C. auris* (from 11 to 27 μg/mL).

Possibly, the duplicated H value, μHrel magnitudes, and its direction totally opposed to Arg residues of the cyclic CysCysCm-p5 (Figure 3) together with the salt bridge substitution by a disulfide bond favored the antifungal activity. In general, these results represent a significant improvement, taking in consideration that this derivative has a stable α-helix structure, which is less dependent on a membrane-mimetic environment, and, consequently, a more effective approach to the fungal membrane.

This peptide has the ability to change between a β-sheet and a helical conformation (according to CD spectra); therefore, it may have the chameleonic possibility to penetrate the membrane as a helix and/or interact with another membrane receptor as a β-sheet. Since the original Cm-p5 acts in a fungistatic manner against *Candida albicans*,[16] a possible complementary therapeutic approach could be conceived and implemented, similar to the combination of fluconazole and amphotericin B,[43] taking into account that resistance to fluconazole increased dramatically in the past years.[44]

Antimicrobial peptides are prone to proteolytic degradation,[45] and MIC determination in standard Mueller-Hinton broth may not always lead to optimal results regarding the

DOI: 10.1021/acsomega.9b02201
ACS Omega XXXX, XXX, XXX−XXX

determination of their antimicrobial activity.[46] To assess the activity of Cm-p5 and its derivatives, we used a modified agar overlay assay[47] and standard MIC determinations (Table 5). In these experiments, we observed a marked increase in the antibacterial activity against Gram-positive and Gram-negative bacteria mostly for the antiparallel derivative.

While the strains included in this investigation (*L. monocytogenes* and *P. aeruginosa*) are not multidrug-resistant microorganisms, it should be noted that *L. monocytogenes* is a major problem in food production due to its ability to multiply at 4 °C and tolerance of high salt concentrations. It can reproduce inside eukaryotic cells and is one of the most serious foodborne pathogens. The 20−30% of listeriosis cases are produced by food, and fatality for high-risk individuals is not uncommon.[48] On the other hand, *P. aeruginosa* is an opportunistic microorganism causing dangerous infection most often in immune-compromised patients or patients with pre-existing diseases like severe burns. In these patients, severe infections and sepsis may frequently be fatal.[49]

Other antibacterial peptides increased their activity when contained in a cycled structure. Bactenecin is a natural antibacterial peptide from bovine neutrophils, which contains a disulfide bond due to two Cys residues.[50] This peptide with such a cycled structure showed a relevant activity against the Gram-negative bacteria *Escherichia coli*, *Pseudomonas aeruginosa*, and *Salmonella typhimurium*. When linear analogues were generated, the antibacterial (Gram-negative) activity decreased substantially, whereas against Gram-positive microorganisms (*Staphylococcus epidermidis* and *Enterococcus faecalis*), these peptide versions displayed a positive interaction. Another example of cyclic peptides with antibacterial activity is gramicidin S, a cationic cyclic decapeptide with primary structure cyclo-(Val-Orn-Leu-D-Phe-Pro)$_2$, which is secreted by the bacterium *Brevibacillus brevis*, is a potent antimicrobial agent at micromolar concentrations, exhibiting high killing activity against a broad spectrum of both Gram-positive and Gram-negative bacteria and pathogenic fungi.[51]

The CysCysCm-p5 cyclic monomer and the two related dimers resulted nontoxic in terms of cell viability, as previously evaluated on human cells (Chart 2). Primary macrophages[52] and the cell line THP-1[53] have been previously used as in vitro cellular models for testing the toxicity of antimicrobial peptides, and they have been proved to be sensitive enough to assess the availability of these molecules as potential anti-infectious drugs in humans. Further experiments with fetal lung cells and determination of cell vitality certainly will improve this analysis, but, for now, it is notable that even at the highest tested concentration, the new compound is not cytotoxic for human cells. Besides Cm-p5 proved nonhemolytic for human and rabbit erythrocytes,[16] the absence of such activity for the CysCysCm-p5 cyclic monomer and the two related dimers, in terms of pharmacological and therapeutic standards for a possible anti-infective candidates, remains to be confirmed.

CONCLUSIONS

Fourteen mutants of the Cm-p5 peptide were synthesized. If other factors such as repulsion of positive charges or loss of noncovalent interaction are present, then maintaining H, μHrel, or the direction of μHrel is not sufficient for maintaining the biological activity. Notable examples constitute all the variants where either Glu4 or His8 was mutated, in which antifungal activity was lost. Substitution of these two residues with Cys allowed us to synthesize a new cyclic analogue and two dimers that showed helix stabilization as indicated by CD analysis and molecular dynamic simulations, suggesting the essential role of the Glu−His salt bridge. For the first time, to our knowledge, it is proposed that a salt bridge can be used as a stabilizing factor for an antimicrobial peptide. CysCysCm-p5 and related dimers were not toxic for human macrophages. The cyclic monomer showed an increased activity in vitro against *C. albicans* and *C. parapsilosis* but not against *C. auris* compared to Cm-p5. In addition, the antiparallel dimer (dimer 2) showed a moderate antibacterial activity against *Pseudomonas aeruginosa* and a significant activity against *Listeria monocytogenes*.

It is important to note that helical stabilization is necessary for biological activity but not sufficient since dimers (more helical character) have lower antifungal activity than Cm-p5 and the parallel version (the most helical-stabilized compound) did not show any antibacterial activity against the tested microbes. The cyclic monomer changes between β-strand and helical conformation when submitted to a membranolytic environment, and the antiparallel dimer (dimer 2) has an equal population of molecules as the β-strand besides having a stabilized α-helix (as judged by CD). Apparently, a constricted helix is not recommended, and a β-strand/α-helix equilibrium in cyclic monomers is needed for antifungal activity. This suggests that an induced-fit model of action mechanism could be better than the old key-lock model to explain the antifungal activity. These peptides may need several conformations to be active because they have several stages in their mechanism of action: interact, penetrate and/or leave the membrane, and interact with the active site of several macromolecular targets.

Finally, the increased capacity of cyclic CysCysCm-p5 for fungal control compared to fluconazole,[17] low cytotoxicity, together with a stabilized α-helix and disulfide bridges, that could advance the metabolic stability, and in vivo activity improve the prospect of this new compound as a potential antifungal systemic therapeutic candidate. Direct application of cyclic CysCysCm-p5 or in synergy with amphotericin B should diminish the doses of this fungicidal compound and is highly toxic but fundamental for the treatment of internal infections.

EXPERIMENTAL SECTION

Materials. All reagents and solvents were obtained from commercial suppliers and used without further purification. Fmoc-Rink-MBHA-Polystyrene and Fmoc-Rink-ChemMatrix resins were prepared by reaction of Fmoc-Rink-OH linker with commercial MBHA-Polystyrene or ChemMatrix resins following controlled acetylation after 0.53 or 0.43 mmol/g substitution, respectively. All the Fmoc-amino acids, DIEA, I_2, ascorbic acid, Ac_2O, and resins were purchased from Merck. Organic solvents (analytical grade) (DMF, CH_2Cl_2, MeOH, Et_2O, and CH_3CN) were purchased from Merck. RP-HPLC quality acetonitrile (CH_3CN) and ultrapure water quality were used for RP-HPLC analysis and purification.

Peptide Synthesis. All reactions were carried in polypropylene plastic syringes (10 mL) fitted with polypropylene frits at room temperature with mechanical shaking, and excess of solvent and reagent was eliminated by vacuum filtration. The side chain of amino acids was protected with Pbf for Arg, Trt for Gln, Cys and His, tBu for Ser and Glu, and Acm for Cys in the synthesis of the parallel dimer (dimer 1).

Solid phase peptide synthesis was carried out using Fmoc/*t*-Bu chemistry on rink amide resin based on polystyrene or PEG (ChemMatrix). The resin was washed with DMF (2 × 2 mL, 1 min), DCM (2 × 2 mL, 1 min), MeOH (2 × 2 mL, 1 min), DCM

DOI: 10.1021/acsomega.9b02201
ACS Omega XXXX, XXX, XXX−XXX

(2 × 2 mL, 1 min), and DMF (2 × 2 mL, 1 min). Fmoc removal was achieved with 20% piperidine in DMF (2 × 10 min), and the subsequent amino acids were added using the following coupling condition: Fmoc-Aa-OH/DIC/Oxyma (4 equiv of each) in DMF after negative ninhydrin test (approximately 30 min). Between the different steps, the resin was washed with DMF (4 × 1 min). Acetylation was achieved using the following condition: Ac_2O/DIEA (8 equiv) in DMF for 10 min.

After the last coupling reaction, Fmoc is eliminated, and peptide-resin is washed subsequently with DMF (4 × 1 min), MeOH (4 × 1 min), and Et_2O (4 × 1 min). Peptide-resin is dried in a desiccator for 3 days and finally frozen at −20 °C for 30 min before cleavage.

All peptides were obtained with more than 95% of purity as ascertained by analytical RP-HPLC. The molecular mass determined experimentally by ESI-MS corresponded with the theoretically calculated monoisotopic mass for each peptide.

Peptide Cleavage. Cleavage from the resin and global deprotection, (i) analogues 1−17: TFA/TIS/H_2O (95:2.5:2.5; 5 mL/g of resin) and (ii) thiolated analogues: TFA/TIS/EDT/H_2O (94:1:2.5:2.5; 5 mL/g of resin), was added to the frozen peptide-resin and left for 2 h with shaking. Cleavage mixture was filtered and added over cold Et_2O (50 mL and −70 °C), mixed in a vortex, and centrifuged. The supernatant was discarded, and the operation was repeated two more times. The solid residue was re-dissolved in H_2O/CH_3CN (7:3), frozen at −70 °C, and lyophilized (LABCONCO, EUA).

Approximately 70% of crude peptide with respect to substitution resin is obtained. Working with 0.3 g of resin, at 0.53 mmol/g substitution for polystyrene resin, and taking into account approximately the range of molar mass of all peptide (1400−1500 g/mol), 160 mg of crude peptides was produced.

In the case of ChemMatrix dimer synthesis, we used 0.15 g of resin and yields of crude are only about 60%, and given the doubleCm-p5 molar mass of product, plus Lys residue (3092 g/mol), 119 mg of crude was produced.

Peptide Cyclization and Dimerization. Cyclization was conducted by dissolving the peptides crude (approximately 160 mg) in H_2O (0.1% TFA)/CH_3CN/*i*-PrOH (1:1:1) at 0.5 mM guaranteeing the major cone of agitation and ball filled only halfway to guarantee a high contact of air (O_2)/solvent. Normally, 250 mL of solvent mixture was used in a necked flask of 1 L.

NH_3 (ac) (25%) was added until pH 8−9, and the reaction was stirred for 4−12 h (after consumption of the staring material, checked by RP-HPLC or HR-MS-ESI) at room temperature. The pH was brought to 7, the H_2O/CH_3CN/*i*-PrOH mixture was removed by a rotary evaporator, and the residue was lyophilized (LABCONCO, EUA).

Cyclization of the Parallel Dimer (Dimer 1) Using Cys(Acm). Peptides (150 mg) containing Cys(Acm) and free Cys in the first or the second Cys residue were submitted to dimerization at high concentrations in 30 mL of DMF/H_2O (1:1) for 72 h (as ascertained by analytical RP-HPLC) in which the formation of white suspension is observed. Subsequently, H_2O (0.1% TFA)/MeOH (1:1) (VT = 250 mL) was added after (0.5 mM). Finally, 1.5 equiv of HCl (37%) (pH = 3,78) and 5 equiv of I_2 (dissolved in MeOH) by the Acm group were supplemented, and stirring was maintained over 3 h or until no dimeric staring material remaining by RP-HPLC. Iodine was removed by adding 1 M aq sodium thiosulfate dropwise until the mixture is colorless or by treatment with activated charcoal and centrifugation. The pH was brought to 7 and the H2O/MeOH mixture was removed by rotary evaporator and residue was lyophilized (LABCONCO, EUA).

Analytical RP-HPLC. Analytical HPLC was performed on an WellChrom HPLC (KNAUER, Germany) using the EZChrom-Elite chromatography software ChromGate v3.1 from Agilent (USA) using a Zorbax RP-C18 (5 μm, 4.6 × 150 mm) column with a flow rate of 0.8 mL/min and UV detection at 226 nm. The mobile phase with a gradient of 5% to 60% B in 35 min was used (solvent A: 0.1% TFA in H_2O; solvent B: 0.1% TFA in CH_3CN). Chromatograms were obtained at 226 nm and processed by the UNICORN 4.11 (GE Healthcare USA) software package.

HR-ESI-MS. Low-energy HR-ESI-MS spectra were obtained by using a hybrid quadrupole time-of-flight QTOF-2 instrument (Waters, Milford, MA, USA) fitted with a nanospray ion source at the CIGB in positive ion mode. Peptide solutions were collected from RP-HPLC, dissolved in 1 mL of 60% (v/v) acetonitrile/water solution containing 0.2% formic acid, and loaded into a metal-coated borosilicate capillary nanotip (Proxeon, Denmark) inserted into the Z-spray nanoflow electrospray ion source and slightly pressured with nitrogen to guarantee their stable spray during the measurement. The capillary and cone voltage were set to 900 to 1200 and 35 V, respectively. Mass spectra were acquired in the m/z range of 400−2000 Th. Electrospray ionization mass spectrometry spectra was processed using the MassLynx version 4.1 program (Micromass, England).

Semipreparative RP-HPLC. Crude peptides (directly cleaved or cyclized) (50 mg for run or 100 mg in the case cyclized crude because it contains approximately 50% of NH_4CF_3COO) were dissolved in DMSO (3 mL) and purified on a LaChrom (Merck Hitachi, Germany) HPLC system using an RP C18 column (Vydac, 25 × 250 mm, 25 μm). A linear gradient from 15 to 60% over 55 min or 25 to 60% of solvent B over 65 min and a flow rate of 5 mL/min were used for linear peptides and cyclic and dimeric analogues, respectively. Detection was accomplished at 226 nm. Solvent A: 0.1% (v/v) of TFA in water. Solvent B: 0.05% (v/v) of TFA in acetonitrile.

Fractions of high HPLC homogeneity and with the expected mass were combined, lyophilized, and submitted to antimicrobial testing. All peptides synthesized showed a purity of >95% by HPLC (see the Supporting Information for chromatograms). Purity, HRMS, and RP-HPLC data are presented in the Supporting Information.

CD Spectroscopy. The CD measurements were made on a J-1500 CD spectrometer (Jasco, Tokyo, Japan) at 24 °C in a thermally controlled quartz cell with a 1 mm path length over 190 to 250 nm. The samples were prepared by dissolving the peptides in water and 10% SDS/water mixture. The final peptide concentration for the CD measurements was ∼35−70 μM (100 μg/mL). Data were collected every 0.1 nm, the bandwidth was set at 1.0 nm, and the sensitivity was 10,000 mdeg. The data integration time was 1 s, and the scanning speed was 100 nm/min. The number of accumulations was 18% of the secondary structure calculated with the Bestsel online program, which is available at the http://bestsel.elte.hu server.[54]

Microorganism Strains and Growth Conditions. Three Candida species were used: *Candida albicans* (ATCC 24433) was obtained from the Institute of Medical Microbiology and Hygiene, University Clinic of Ulm, Germany. *Candida parapsilosis* (ATCC 22019) was obtained from the laboratory of Medical Mycology, "Pedro Kourí" Institute of Tropical Medicine, Havana Cuba; *Candida auris* (DSMZ-No. 21092,

DOI: 10.1021/acsomega.9b02201
ACS Omega XXXX, XXX, XXX−XXX

CBS 10913, and JCM 15448)[55] was obtained from the Leibniz Institute DSMZ-German Collection of Microorganisms and Cell Cultures.

Yeast extract−peptone−dextrose (YPD) medium (liquid) was used for pre-culture inoculum at 70 rpm agitated conditions at 37 °C for 24 hours.

Trichophyton rubrum (ATCC 28189) was obtained from the American Type Culture Collection and cultured in potato dextrose agar and for inoculums in Roswell Park Memorial Institute (RPMI) 1640 Medium.

Two bacteria genera were used: *Listeria monocytogenes* (ATCC BAA-679/EGD-e) and *Pseudomonas aeruginosa* (ATCC 27853). Bacteria were cultured at 37 °C/5%CO_2 overnight as pre-culture inoculum in culture media.

In Vitro Antimicrobial Testing. For *Candida* species and *T. rubrum*, the minimal inhibitory concentration (MIC) of Cm-p5 derivatives (cyclic monomer and the two dimers) was determined according to the "Clinical and Laboratory Standards Institute" guidelines M27-A3 broth microdilution assay[56] with modifications (turbidimetric detection). Based on cell density measurements, the MIC was derived from a Lambert−Pearson plot.[57] Flat-bottomed sterile 96-well plates (SARSTEDT, AG & Co KG, Nümbrecht), RPMI 1640 without sodium bicarbonate, MOPS-buffered (Sigma-Aldrich-Merck, Darmstadt) were used for the test, and readings were performed at λ = 600 nm with a TECAN infinite M200 microplate reader (Tecan Group Ltd., Männedorf). For filamentous fungi, the minimal inhibitory concentration was determined according to CLSI guidelines M38-A2.[48]

For bacteria genera:

1. Agar overlay assay: Bacteria were cultured at 37 °C/5% CO_2 overnight, pelleted by centrifugation, and washed in 10 mM sodium phosphate buffer. Following resuspension in 10 mM sodium phosphate buffer, optical density was determined at 600 nm. Bacteria (2×10^7) were seeded into a Petri dish in 1% agarose and 10 mM sodium phosphate buffer. After cooling at 4 °C for 30 min, 3−5 mm holes were punched into the 1% agarose. Peptides adjusted to the desired concentration in 10 μL of buffer were filled into the agar holes. Following and incubation at 37 °C in ambient air for 3 h, plates were overlaid with 1% agarose and tryptic soy solved in 10 mM phosphate buffer. Inhibition zones in mm were determined following 16−18 h incubation time at 37 °C/5% CO_2.[47]
2. Minimal inhibitory concentration (MIC) determination: MIC determinations were performed in Mueller Hinton broth according to CLSI reference method M7A9 with modifications for bacteria.[49] All tests were performed in triplicate.

Human Cells and Culture Conditions. For hMDMs (human monocyte-derived macrophages), peripheral blood mononuclear cells (PBMCs) were isolated from human buffy coat via high density gradient centrifugation (Ficoll-Paque Plus; GE Healthcare, Munich). Monocytes were then purified from the PBMCs through adherence. Then, the cells were stimulated with granulocyte macrophage colony-stimulating factor (GM-CSF) (10 ng/mL; MiltenyiBiotec, BergischGladbach) for 6 days at 37 °C and 5% CO_2 in RPMI 1640 medium (GIBCO, Invitrogen, Munich) supplemented with 2 mM L-glutamine (PAN Biotech, Aidenbach), 10 mM HEPES (Biochrom, GmbH, Berlin), and penicillin/streptomycin (100 U mL^{-1}/100 $\mu g\ mL^{-1}$ (Biochrom, GmbH, Berlin).

For the THP-1 cell line (ECACC, Porton Down, UK, 88081201), human monocytic cell line derived from an acute monocytic leukemia patient was differentiated to macrophage-like cells in the cell culture medium. Mercaptoethanol (0.05 mM; Sigma, Merck KGaA, Darmstadt), 10% FCS (Biochrom, GmbH, Berlin), and phorbol 12-myristate 13-acetate (PMA) (1 μg/mL; Sigma, Merck KGaA, Darmstadt) were used as supplemented at 36 °C/5%CO_2 overnight.

Toxicity Assay. macrophages/THP-1 cells per well (1×10^5) were distributed into a microplate (Nunclon Delta 96-well MicroWell Plates, sterile, Thermo Scientific, Germany) in the cell culture medium supplemented with 5% heat-inactivated human serum (PAN Biotech, Aidenbach). Controls were media control, heat-inactivated cells, and diluent control, dimethylsulfoxide (DMSO; Carl Roth, Karlsruhe). Cells were then stimulated with the Cm-p5 derivatives in different concentrations overnight. A 20 μL PrestoBlue Cell Viability Reagent (Thermo Fisher Scientific Life Technologies GmbH, Darmstadt) per well was added for 20 min at 37 °C/ 5%CO_2. The fluorescence was measured at an excitation of 560 nm and emission of 600 nm with the TECAN infinite M200 microplate reader (Tecan Group Ltd., Männedorf). The optical density (OD) of the media control was then subtracted from other results. Unstimulated cells were set to 100% viability.

Molecular Dynamic Simulations. Distance between S−S was determined for the N-terminal acetylated peptide Ac-SRSCLIVCQRLF-NH_2 in order to avoid electrostatic effects of the amine group, and the molecule was fully solvated in an octahedral box of TIP3P water model with periodic boundary conditions. The MDS was performed using AM-BER 11 (http://infoscience.epfl.ch/record/150146/files/Amber11.pdf?version=1).[58] The model was prepared with a three-step protocol. We first ran 2000 steps of side-chain optimization, then 50,000 steps of thermalization at 300 K with a Berendsen thermostat at constant volume, and third, 50,000 steps at the same temperature with constant pressure (isotropic position scaling) of 1 atm. Finally, we performed a 50 ns of MDS under the NPT ensemble condition.

Estimation of α-helix contents were performed for the native peptide Cm-p5 (2MP9) and the cyclic and dimers of CysCysCm-p5 (Supplementary Data 2). For each system, two 50 ns simulations, at 310 K, were performed using the GROMOS96 force field;[59] one in pure water and one in 40% (v/v) TFE/water. In Table 4, the composition of the simulated systems is reported.

α-Helix content calculations were computed with DSSP.[60] The percentage of α-helix is calculated on all peptide residues.

■ ASSOCIATED CONTENT

Supporting Information

The Supporting Information is available free of charge on the ACS Publications website at DOI: 10.1021/acsomega.9b02201.

Experimental procedures, RP-HPLC chromatograms, and ESI-HRMS spectra of all final compounds (SD1) and molecular dynamic simulation description (SD2) (PDF)

Molecular formula strings (CSV)

■ AUTHOR INFORMATION

Corresponding Authors

*E-mail: marelloweber@gmail.com (W.P.).

*E-mail: ludger.staendker@uni-ulm.de (L.S.).

DOI: 10.1021/acsomega.9b02201
ACS Omega XXXX, XXX, XXX−XXX

*E-mail: aotero@fbio.uh.cu (A.J.O.-G.).

ORCID

Daniel G. Rivera: 0000-0002-5538-1555
Rosemeire C. L. R. Pietro: 0000-0001-7859-8127
Frank Rosenau: 0000-0002-9297-6419
Márcio Weber Paixão: 0000-0002-0421-2831
Ludger Ständker: 0000-0002-8436-4260

Author Contributions

The authors contributed equally to this paper. The manuscript was written through contributions of all authors. All authors have given approval to the final version of the manuscript.

Funding

This work was funded in part by the German Federal Ministry of Education and Research (BMBF) project (DLR CUB 17WTZ-014/01DN18009), the German Research Society (DFG) project CRC1279 (Exploiting the Human Peptidome for Novel Antimicrobial and Anticancer Agents), and CAPES Funding Sources, Brazil.

Notes

The authors declare no competing financial interest.

■ ACKNOWLEDGMENTS

The authors thank the Laboratory of Synthetic Peptides, Center for Genetic Engineering and Biotechnology, La Habana, Cuba, and Laboratory of Pharmaceutical Biotechnology, Department of Drugs and Medicines, School of Pharmaceutical Sciences, UNESP, Araraquara, Brazil.

■ REFERENCES

(1) Amábile-Cuevas, C. Society must seize control of the antibiotics crisis: pressure from the public could force firms to develop new drugs that treat resistant infections. *Nature* **2016**, *533*, 439.

(2) Arias, C. A.; Murray, B. E. Antibiotic-Resistant Bugs in the 21st Century — A Clinical Super-Challenge. *N. Engl. J. Med.* **2009**, *360*, 439−443.

(3) (a) Alonso, R.; Pisa, D.; Marina, A. I.; Morato, E.; Rábano, A.; Rodal, I.; Carrasco, L. Evidence for Fungal Infection in Cerebrospinal Fluid and Brain Tissue from Patients with Amyotrophic Lateral Sclerosis. *Int. J. Biol. Sci.* **2015**, *11*, 546−558. (b) Alonso, R.; Pisa, D.; Fernández-Fernández, A. M.; Rábano, A.; Carrasco, L. Fungal Infection in neural tissue of patients with amyotrophic lateral sclerosis. *Neurobiol Dis.* **2017**, *108*, 249−260. (c) Alonso, R.; Pisa, D.; Fernández-Fernández, A. M.; Carrasco, L. Infection of Fungi and Bacteria in Brain Tissue From Elderly Persons and Patients With Alzheimer's Disease. *Front. Aging Neurosci.* **2018**, *10*, 159.

(4) (a) Huang, R.; Li, M.; Gregory, R. L. Bacterial interactions in dental biofilm. *Virulence* **2014**, *2*, 435−444. (b) Akyıldız, İ.; Take, G.; Uygur, K.; Kızıl, Y.; Aydil, U. Bacterial Biofilm Formation in the Middle-Ear Mucosa of Chronic Otitis Media Patients. *Indian J. Otolaryngol. Head Neck Surg.* **2013**, *65*, 557−561.

(5) Cunha, B. A. Antibiotic side effects. *Medical Clinics of North America* **2001**, *85*, 149−185.

(6) Kumar, P.; Kizhakkedathu, J.; Straus, S. Antimicrobial Peptides: Diversity, Mechanism of Action and Strategies to Improve the Activity and Biocompatibility in Vivo. *Biomolecules* **2018**, *8*, 4.

(7) Hancock, R. E. W.; Haney, E. F.; Gill, E. E. The immunology of host defence peptides: beyond antimicrobial activity. *Nat. Rev. Immunol.* **2016**, *16*, 321−334.

(8) Hossen, M. S.; Gan, S. H.; Khalil, M. I. Melittin, a Potential Natural Toxin of Crude Bee Venom: Probable Future Arsenal in the Treatment of Diabetes Mellitus. *J. Chem.* **2017**, 1−7.

(9) Porto, W. F.; Irazazabal, L.; Alves, E. S. F.; Ribeiro, S. M.; Matos, C. O.; Pires, Á. S.; Fensterseifer, I. C. M.; Miranda, V. J.; Haney, E. F.; Humblot, V.; Torres, M. D. T.; Hancock, R. E. W.; Liao, L. M.; Ladram, A.; Lu, T. K.; de la Fuente-Nunez, C.; Franco, O. L. In silico optimization of a guava antimicrobial peptide enables combinatorial exploration for peptide design. *Nat. Commun.* **2018**, *9*, 1490.

(10) Vijayaraghavan, R.; Mathian, V. M.; Sundaram, A. M.; Karunakaran, R.; Vinodh, S. Triple antibiotic paste in root canal therapy. *J. Pharm. BioAllied Sci.* **2012**, *4*, S230−S233.

(11) Henninot, A.; Collins, J. C.; Nuss, J. M. The Current State of Peptide Drug Discovery: Back to the Future ? *J. Med. Chem.* **2018**, *61*, 1382−1414.

(12) Sewald, N.; Jakubke, H. D. *Peptides: Chemistry and Biology*. Wiley-VCH Verlag GmbH & Co. KGaA: Weinheim, Germany, 2002.

(13) López-Abarrategui, C.; Alba, A.; Silva, O. N.; Reyes-Acosta, O.; Vasconcelos, I. M.; Oliveira, J. T. A.; Migliolo, L.; Costa, M. P.; Costa, C. R.; Silva, M. R. R.; Garay, H. E.; Dias, S. C.; Franco, O. L.; Otero-González, A. J. Functional characterization of a synthetic hydrophilic antifungal peptide derived from the marine snail *Cenchritis muricatus*. *Biochimie* **2012**, *94*, 968−974.

(14) Sun, Z. J.; Heffron, G.; Mcbeth, C.; Wagner, G.; Otero-González, A. J.; Starnbach, M. N., *Solution structure of a potent antifungal peptide Cm-p5 derived from C. muricatus*. Deposit PDB: 2014-05-14, Status HPUB, entrance code 2MP9, 2014.

(15) López-Abarrategui, C.; McBeth, C.; Mandal, S. M.; Sun, Z. J.; Heffron, G.; Alba-Menéndez, A.; Migliolo, L.; Reyes-Acosta, O.; García-Villarino, M.; Nolasco, D. O.; Falcão, R.; Cherobim, M. D.; Dias, S. C.; Brandt, W.; Wessjohann, L.; Starnbach, M.; Franco, O. L.; Otero-González, A. J. Cm-p5: an antifungal hydrophilic peptide derived from the coastal mollusk Cenchritis muricatus (Gastropoda: Littorinidae). *FASEB J.* **2015**, *29*, 3315−3325.

(16) González-Garcia, M.; Valdés, M. E.; Freitas, C. G.; Menéndez, A. A.; López-Abarrategui, C.; San Juan-Galán, J.; Campos Diaz, S.; Luiz Franco, O.; Otero-González, A. J. In vitro complementary biological activity of the antifungal peptide Cm-p5 and in silico prediction of its functional regions. *Rev Cubana Med Tropical* **2017**, *69*, 1−15.

(17) (a) Clancy, C. J.; Yu, V. L.; Morris, A. J.; Snydman, D. R.; Nguyen, M. H. Fluconazole MIC and the Fluconazole Dose/MIC Ratio Correlate with Therapeutic Response among Patients with Candidemia. *Antimicrob. Agents Chemother.* **2005**, *49*, 3171−3177. (b) Szabó, Z.; Sóczó, G.; Miszti, C.; Hermann, P.; Rozgonyi, F. In vitro activity of fluconazole and amphotericin B against Candida inconspicua clinical isolates as determined by the time-kill method. *Acta. Microbiol. Immunol. Hung.* **2008**, *55*, 53−61.

(18) Schmidt, N. W.; Mishra, A.; Lai, G. H.; Davis, M.; Sanders, L. K.; Tran, D.; Garcia, A.; Tai, K. P.; McCray, P. B., Jr.; Ouellette, A. J.; Selsted, M. E.; Wong, G. C. L. Criterion for Amino Acid Composition of Defensins and Antimicrobial Peptides Based on Geometry of Membrane Destabilization. *J. Am. Chem. Soc.* **2011**, *133*, 6720−6727.

(19) Vazquez, J. A. Anidulafungin: A new echinocandin with a novel profile. *Clin Ther.* **2005**, *27*, 657−673.

(20) Ghannoum, M. A.; Rice, L. B. Antifungal Agents: Mode of Action, Mechanisms of Resistance, and Correlation of These Mechanisms with Bacterial Resistance. *Clin. Microbiol. Rev.* **1999**, *12*, 501−517.

(21) Elewski, B. E. Mechanisms of action of systemic antifungal agents. *J. Am. Acad. Dermatol.* **1993**, *28*, S28−S34.

(22) Edelheit, O.; Hanukoglu, I.; Dascal, N.; Hanukoglu, A. Identification of the roles of conserved charged residues in the extracellular domain of an epithelial sodium channel (ENaC) subunit by alanine mutagenesis. *Am. J. Physiol. Renal Physiol.* **2011**, *300*, F887−F897.

(23) Marcos, J. F.; Muñoz, A.; Pérez-Payá, E.; Misra, S.; López-García, B. Identification and Rational Design of Novel Antimicrobial Peptides for Plant Protection. *Annu. Rev. Phytopathol.* **2008**, *46*, 273−301.

(24) Helmerhors, E. J.; Breeuwer, P.; Van't Hof, W.; Walgreen-Weterings, E.; Oomeni, L. C. J. M.; Veerman, E. C. I.; Amerongen, A. V. N.; Abee, T. The Cellular Target of Histatin 5 onCandida albicansIs the Energized Mitochondrion. *J. Biol. Chem.* **1999**, *274*, 7286−7291.

(25) Epand, R. M.; Vogel, H. J. Diversity of antimicrobial peptides and their mechanisms of action. *Biochim. Biophys. Acta* **1999**, *1462*, 11−28.

DOI: 10.1021/acsomega.9b02201
ACS Omega XXXX, XXX, XXX−XXX

(26) Chan, D. I.; Prenner, E. J.; Vogel, H. J. Tryptophan- and arginine-rich antimicrobial peptides: Structures and mechanisms of action. *Biochim. Biophys. Acta* **2006**, *1758*, 1184−1202.
(27) Van Loon, L. C.; Rep, M.; Pieterse, C. M. J. Significance of inducible defense-related proteins in infected plants. *Annu. Rev. Phytopathol.* **2006**, *44*, 135−162.
(28) Dathe, M.; Wieprecht, T. Structural features of helical antimicrobial peptides: their potential to modulate activity on model membranes and biological cells. *Biochim. Biophys. Acta* **1999**, *1462*, 71−87.
(29) Eisenberg, D.; Weiss, R. M.; Terwilliger, T. C. The helical hydrophobic moment: a measure of the amphiphilicity of a helix. *Nature* **1982**, *299*, 371−374.
(30) Gautier, R.; Douguet, D.; Antonny, B.; Drin, G. HELIQUEST: a web server to screen sequences with specific -helical properties. *Bioinformatics* **2008**, *24*, 2101−2102.
(31) Tam, J. P.; Lu, Y. A.; Yang, J. L. Antimicrobial dendrimeric peptides. *Eur. J. Biochem.* **2002**, *269*, 923−932.
(32) Dougherty, D. A. Modern Physical Organic Chemistry. *J. Chem. Educ.* **2006**, *83*, 387.
(33) Baker, E. G.; Bartlett, G. J.; Crump, M. P.; Sessions, R. B.; Linden, N.; Faul, C. F. J.; Woolfson, D. N. Local and macroscopic electrostatic interactions in single α-helices. *Nat. Chem. Biol.* **2015**, *11*, 221−228.
(34) (a) Anderson, D. E.; Becktel, W. J.; Dahlquist, F. W. pH-Induced Denaturation of Proteins: A Single Salt Bridge Contributes 3-5 kcal/mol to the Free Energy of Folding of T4 Lysozyme. *Biochemistry* **1990**, *29*, 2403−2408. (b) Horovitz, A.; Serrano, L.; Avron, B.; Bycroft, M.; Fersht, A. R. Strength and Co-operativity of Contributions of Surface Salt Bridges to Protein Stability. *J. Mol. Biol.* **1990**, *216*, 1031−1044.
(35) Mihailescu, E.; Worcester, D.; Castro-Roman, F.; Fernandez-Vidal, M.; White, S. H. Determining the Water Content of Lipid Membranes by Neutron Diffraction. *Biophys. J.* **2010**, *98*, 286A.
(36) Liang, M.-K.; Patwardhan, S. V.; Danilovtseva, E. N.; Annenkov, V. V.; Perry, C. C. Imidazole catalyzed silica synthesis: Progress toward understanding the role of histidine in (bio) silicification. *J. Mater. Res.* **2009**, *24*, 1700−1708.
(37) Henchey, L. K.; Jochim, A. L.; Arora, P. S. Contemporary strategies for the stabilization of peptides in the α-helical conformation. *Curr. Opin. Chem. Biol.* **2008**, *12*, 692−697.
(38) Garay, H.; Espinosa, L. A.; Perera, Y.; Sánchez, A.; Diago, D.; Perea, S. E.; Besada, V.; Reyes, O.; González, L. J. Characterization of low-abundance species in the active pharmaceutical ingredient of CIGB-300: A clinical-grade anticancer synthetic peptide. *J. Pep. Sci.* **2018**, *24*, No. e3081.
(39) (a) Hong, D.-P.; Hoshino, M.; Kuboi, R.; Goto, Y. Clustering of Fluorine-Substituted Alcohols as a Factor Responsible for Their Marked Effects on Proteins and Peptides. *J. Am. Chem. Soc.* **1999**, *121*, 8427−8433. (b) Vymětal, J.; Bednárová, L.; Vondrášek, J. Effect of TFE on the Helical Content of AK17 and HAL-1 Peptides: Theoretical Insights into the Mechanism of Helix Stabilization. *J. Phys. Chem. B* **2016**, *120*, 1048−1059.
(40) Roccatano, D.; Colombo, G.; Fioroni, M.; Mark, A. E. Mechanism by which 2,2,2-trifluoroethanol/water mixtures stabilize secondary-structure formation in peptides: A molecular dynamics study. *PNAS* **2002**, *99*, 12179−12184.
(41) (a) Gimpelev, M.; Forrest, L. R.; Murray, D.; Honig, B. Helical Packing Patterns in Membrane and Soluble Proteins. *Biophys. J.* **2004**, *87*, 4075−4086. (b) Walters, R. F. S.; DeGrado, W. F. Helix-packing motifs in membrane proteins. *PNAS* **2006**, *103*, 13658−13663.
(42) Dalton, J. A. R.; Michalopoulos, I.; Westhead, D. R. Calculation of helix packing angles in protein structures. *Bioinformatics* **2003**, *19*, 1298−1299.
(43) Larsen, R. A.; Bauer, M.; Thomas, A. M.; Graybill, J. R. Amphotericin B and Fluconazole, a Potent Combination Therapy for Cryptococcal Meningitis. *Antimicrob. Agents Chemother.* **2004**, *48*, 985−991.
(44) Richardson, M. D. Changing patterns and trends in systemic fungal infections. *J. Antimicrob. Chemoter.* **2005**, *56*, i5−i11.
(45) Sieprawska-Lupa, M.; Mydel, P.; Krawczyk, K.; Wójcik, K.; Puklo, M.; Lupa, B.; Suder, P.; Silberring, J.; Reed, M.; Pohl, J.; Shafer, W.; McAleese, F.; Foster, T.; Travis, J.; Potempa, J. Degradation of human antimicrobial peptide LL-37 by Staphylococcus aureus-derived proteinases. *Antimicrob. Agents Chemother.* **2004**, *48*, 4673−4679.
(46) Steinberg, D. A.; Lehrer, R. I. Designer assays for antimicrobial peptides. Disputing the ″one-size-fits-all″ theory. *Methods Mol. Biol.* **1997**, *78*, 169−186.
(47) Turner, J.; Cho, Y.; Dinh, N.-N.; Waring, A. J.; Lehrer, R. I. Activities of LL-37, a Cathelin-Associated Antimicrobial Peptide of Human Neutrophils. *Antimicrob. Agents Chemother.* **1998**, *42*, 2206−2214.
(48) Ramaswamy, V.; Cresence, V. M.; Rejitha, J. S.; Lekshmi, M. U.; Dharsana, K. S.; Prasad, S. P.; Vijila, H. M. Listeria−review of epidemiology and pathogenesis. *J. Microbiol. Immunol. Infect.* **2007**, *40*, 4−13.
(49) Balcht, A.; Smith, R. Pseudomonas aeruginosa: Infections and Treatment. *Informa Health Care* **1994**, *2*, 83−84.
(50) Wu, M.; Hancock, R. E. W. Improved derivatives of bactenecin, a cyclic dodecameric antimicrobial cationic peptide. *Antimicrob. Agents Chemother.* **1999**, *43*, 1274−1276.
(51) Ashrafuzzaman, M.; Andersen, O. S.; McElhaney, R. N. The antimicrobial peptide gramicidin S permeabilizes phospholipid bilayer membranes without forming discrete ion channels. *Biochim. Biophys. Acta* **2008**, *1778*, 2814−2822.
(52) Koyama, Y.; Motobu, M.; Hikosaka, K.; Yamada, M.; Nakamura, K.; Saido-Sakanaka, H.; Asaoka, A.; Yamakawa, M.; Isobe, T.; Shimura, K.; Kang, C. B.; Hayashidani, H.; Nakai, Y.; Hirota, Y. Cytotoxicity and antigenicity of antimicrobial synthesized peptides derived from the beetle Allomyrina dichotoma defensin in mice. *Int. Immunopharmacol.* **2006**, *6*, 1748−1753.
(53) Pick, N.; Cameron, S.; Arad, D.; Av-Gay, Y. Screening of Compounds Toxicity against Human Monocytic cell line-THP-1 by Flow Cytometry. *Biol. Proced. Online* **2004**, *6*, 220−225.
(54) Micsonai, A.; Wien, F.; Kernya, L.; Lee, Y.-H.; Goto, Y.; Réfrégiers, M.; Kardos, J. Accurate secondary structure prediction and fold recognition for circular dichroism spectroscopy. *PNAS* **2015**, *112*, E3095−103.
(55) Satoh, K.; Makimura, K.; Hasumi, Y.; Nishiyama, Y.; Uchida, K.; Yamaguchi, H. Candida auris sp. nov., a novel ascomycetous yeast isolated from the external ear canal of an inpatient in a Japanese hospital. *Microbiol. Immunol.* **2009**, *53*, 41−44.
(56) Clinical and Laboratory Standards Institute Reference method for broth dilution antifungal susceptibility testing of yeasts; approved standard In *CLSI document M27-A3*; Wayne: Clinical and Laboratory Standards Institute Third edition 2008; pp 1−25.
(57) Lambert, R. J. W.; Pearson, J. Susceptibility testing: Accurate and reproducible minimum inhibitory concentration (MIC) and non-inhibitory concentration (NIC) values. *J. Appl. Microbiol.* **2000**, *88*, 784−790.
(58) Case, D. A.; Darden, T. A.; Cheatham, T. E.; Simmerling, C. L.; Wang, J. *AMBER11*; University of California: San Francisco, 2010.
(59) Schmid, N.; Eichenberger, A. P.; Choutko, A.; Riniker, S.; Winger, M.; Mark, A. E.; Van Gunsteren, W. F. Definition and testing of the GROMOS force-field versions 54A7 and 54B7. *Eur. Biophys. J.* **2011**, *40*, 843−856.
(60) (a) Kabsch, W.; Sander, C. Dictionary of protein secondary structure: Pattern recognition of hydrogen-bonded and geometrical features. *Biopolymers* **1983**, *22*, 2577−2637. (b) Touw, W. G.; Baakman, C.; Black, J.; te Beek, T. A. H.; Krieger, E.; Joosten, R. P.; Vriend, G. A series of PDB-related databanks for everyday needs. *Nucl. Acids Res.* **2015**, *43*, D364−D368.

DOI: 10.1021/acsomega.9b02201
ACS Omega XXXX, XXX, XXX−XXX